THE ATHLET/BIPR8KN CODE PACKAGE APPLICATION FOR THE CALCULATION OF THE COOLANT PARAMETERS DISTRIBUTION IN THE REACTOR PRESSURE VESSEL.

A.Kotsarev, M.Lizorkin, S.Nikonov
RRC "Kurchatov Institute", Institute of Nuclear Reactors,
VVER Department, Moscow, Russia

ABSTRACT

The questions of intra-reactor vessel modeling with the aim of the calculation of the three- dimensional (coarse mesh) coolant parameters distribution in the reactor pressure vessel within the frame of the ATHLET/BIPR8KN /1/ application are considered. The turning on of the inactive loop of VVER-440 reactor of Kola NPP is presented as an example

The first attempt of the coolant mixing boundaries estimation for the analysis of the process of the turning on of the inactive loop with different temperature or boron concentration with ATHLET/BIPR8KN /2/ code package in use have been made at the AER Working group D meeting in Moscow. In this simplified case, the modeling was made by selection of the pair element for the description of each of the characterized reactor part from the inlet up to the core. These elements were proportional by geometry to the five combined and one-selected loops. All part of the reactor was independent from each other. The mixing (from minimal up to maximal) was modeled in under-core space by given values of the coolant cross flow.

The aim of the simplified investigation was both the receiving of calculated estimation of mixing degree influence on the process and answer on the question: what mixing degree leads to the most conservative results.

The goal of the presented report is to show the use possibility of ATHLET/BIPR8KN code package for the coarse-mesh modeling of the reactor, including the assembly by assembly calculation of the full core from the both hydro-dynamic and neutron kinetic point of view. It is not supported to use the special approaches for the mixing modeling for the receiving the space dependency distribution of the hydrodynamic parameters.

The selection of some different reactor zones is supported by the space grid building Each zone has own spacing out. These zones are:

- Inlet mixing camera with down camera;
- Space between the elliptical reactor bottom and the reactor shaft;
- Space between the elliptical reactor bottom and lower base plate of the reactor shaft;
- Under core space from lower base plate of the reactor shaft up to the lower base plate of the reactor core;
- The core assemblies (each assembly correspond to the separate thermal hydraulic channel, without taking into account the intra-mixing;
- Space between lower and upper kept plate of the emergency cooling down system directing tube;
- Outlet camera;
- Space between upper kept plate of the emergency cooling down system directing tubes and head of the reactor.

Such approach allows refusing from the working out in detail of the parts, which do not have influence on the process and giving possibility to describe in more detail the reactor parts, where the mixing process is essential.

It is supported that all pins of each assembly are equivalent by the heat structure modeling.

The full scheme of the plant (primary side, secondary side) is realized in this calculation in one-dimensional approach.

Conclusion

The principal possibility of the using of the ATHLET/BIPR8KN code package for the tree-dimensional coarse-mesh calculation of the reactor is shown.

The authenticity of such approach applying will be tested on existing experimental data. It will be useful and desirable to have the temperature measurements at the assembly inlet in the process of the inactive loop turning on. Unfortunately, there are not such data.

The increase of the amount of details is limited by the computer memory and processor. It has huge influence at the stage of initial matrix optimization.

To proceed from the carried out calculation with such model in use, the follow preliminary conclusions about the slug mixing degree can be done:

- The slug from the being turned on loop has gone to the reactor vessel bottom without any mixing;
- The main mixing is occurred on the way from reactor vessel bottom up to the hole shield;
- As a result, the slug is fully mixing at the inlet of the core. The mixing degree is close to 100%, then 0%.

The further work by the use of the **ATHLET/BIPR8KN** code package for the three dimensional coarse-mesh modeling of the reactor will concentrate on the verification of such assumption on the base of the experimental data. It should be said, that the three dimensional coarse-mesh model of the steam generator is developed at the time being on the base of the ATHLET program /3/.

Literature

1. S.Danilin, S.Nikonov, M.Lizorkin, The New Solution of the AER Sixth Dynamic Benchmark Problem With ATHLET/BIPR8, Working Groop D meeting, Moscow, Russia, 21-23 May,2002

2. A.Kotsarev, S.Danilin, S.Nikonov, M.Lizorkin, Influence of the mixing degree on the process connected with the wrong start up of the circulation loop, Working Groop D meeting, Moscow, Russia, 21-23 May,2002

3. G.Lerchel, H.Austregesilo, ATHLET Mod1.2 Cycle B, User's Manual,GRS,1999

Appendix.

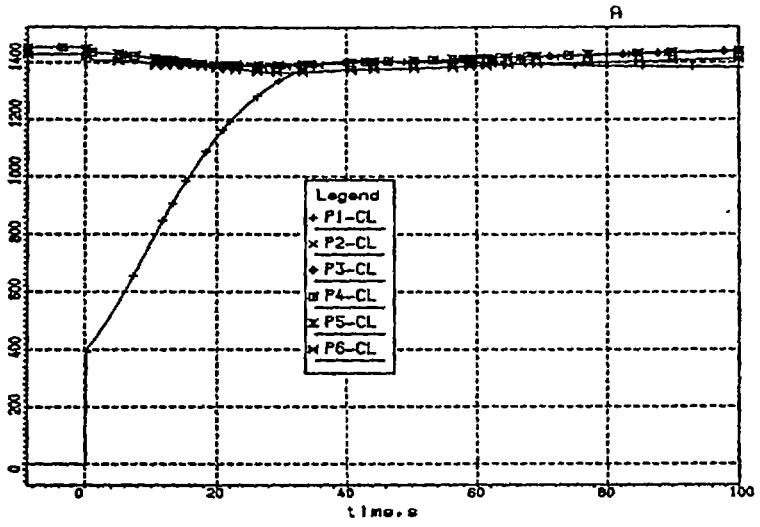

Figure 1. Loop mass flow rate, kg/sec

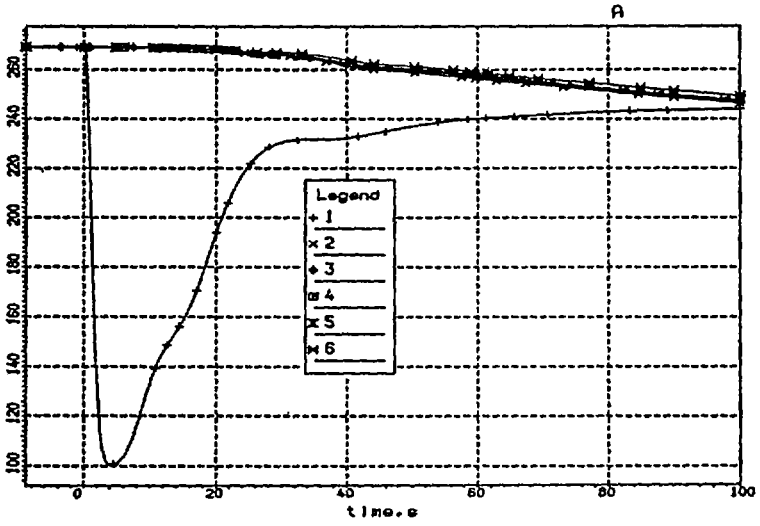

Figure 2. Cold leg outlet temperature, °C

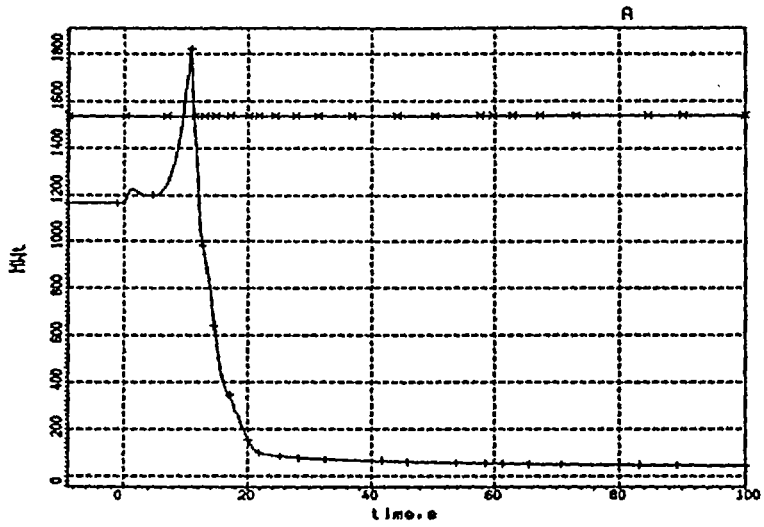

Figure 3. Neutron power (+) and set point of the scram 112% (x).

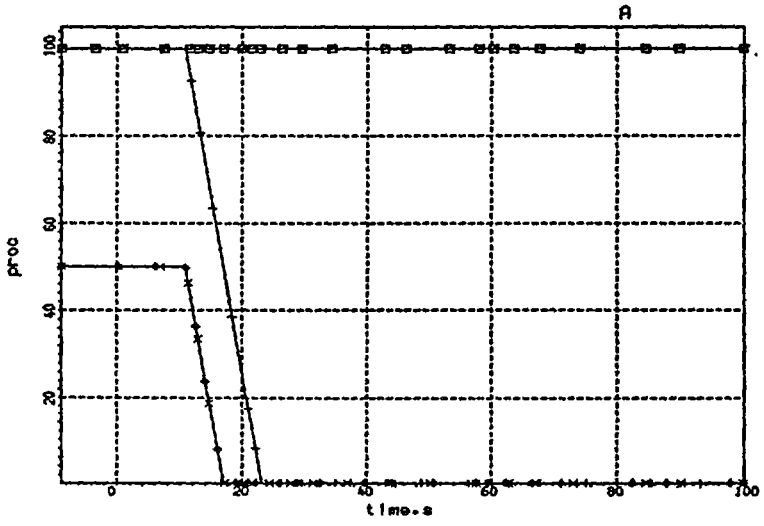

Figure 4. Position of the scram(+), working group(x), (◊) and stuck rod(□)

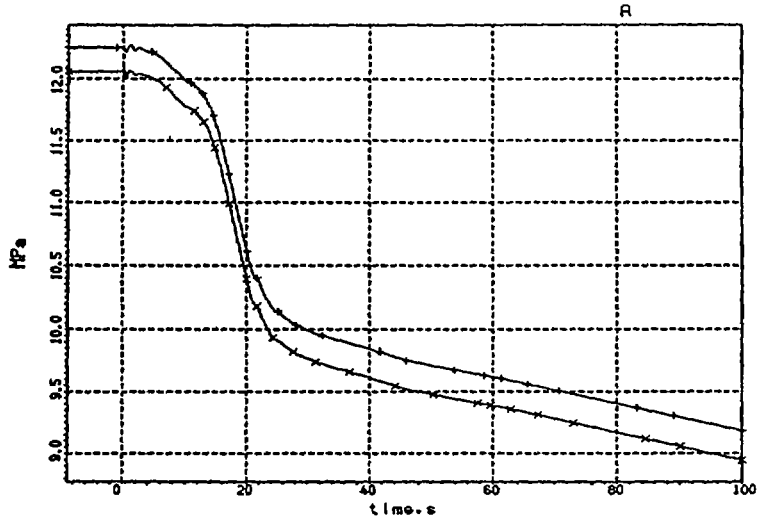

Figure 5. Coolant pressure at the inlet(+) and outlet of the reactor.

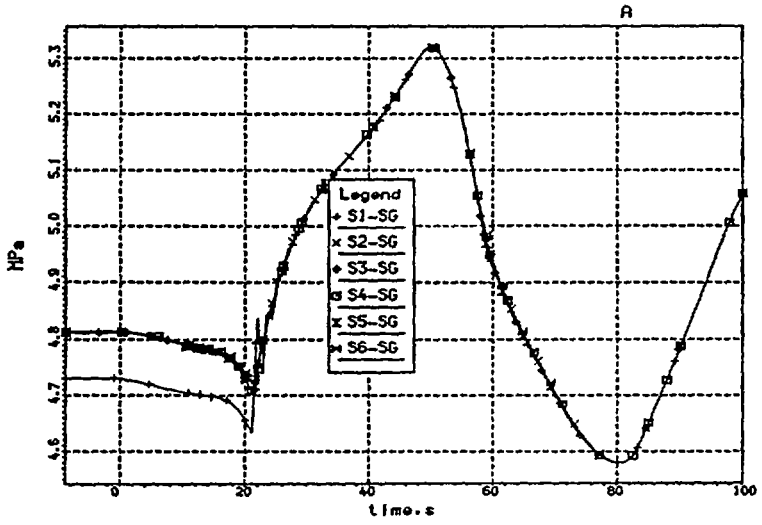

Figure 6. Pressure at the steam generator outlet

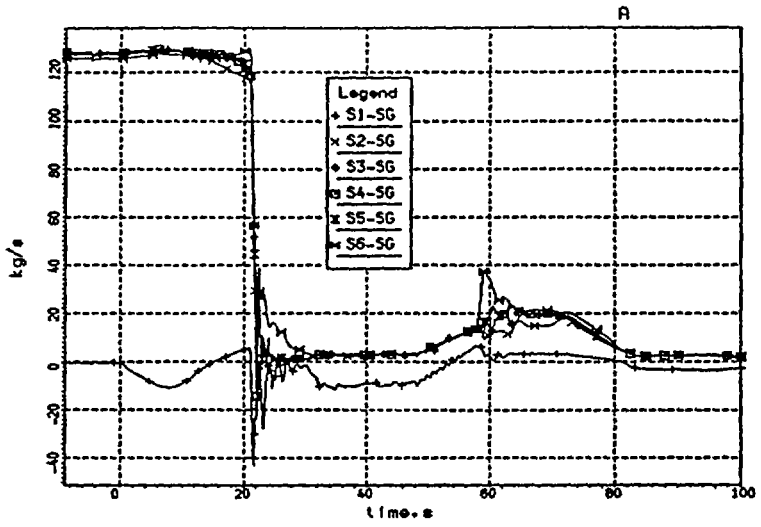

Figure 7. Steam mass flow rate at the steam generator outlet

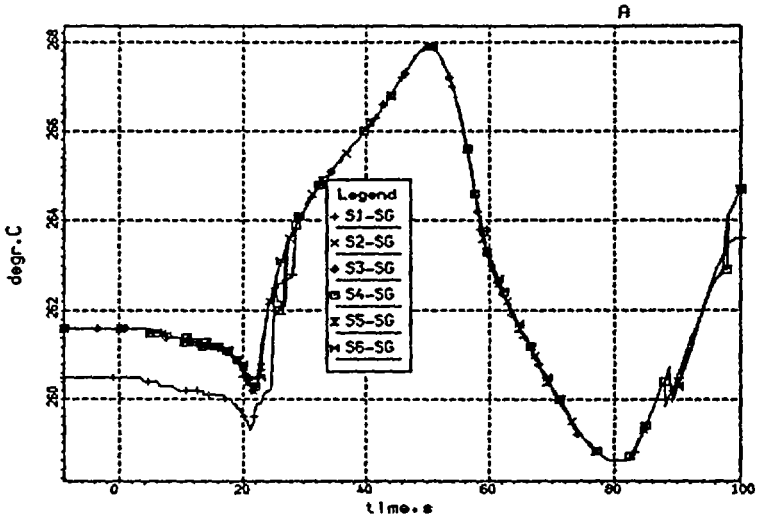

Figure 8. Steam temperature at the steam generator outlet

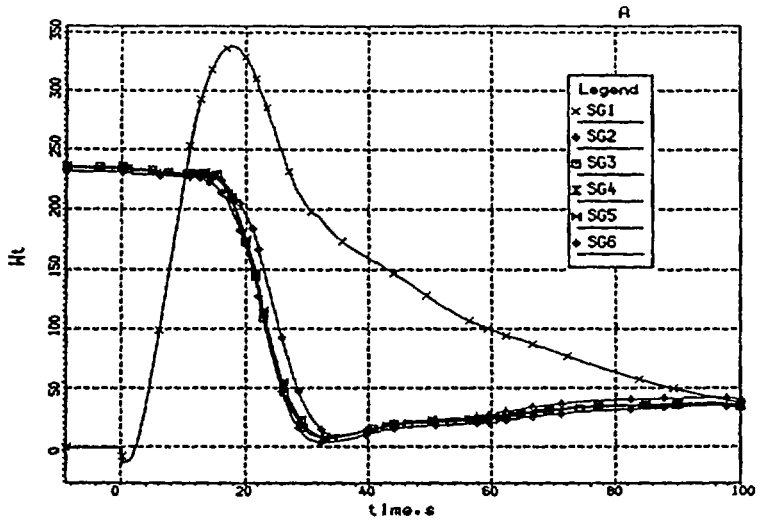

Figure 9. Heat transfer through the steam generators

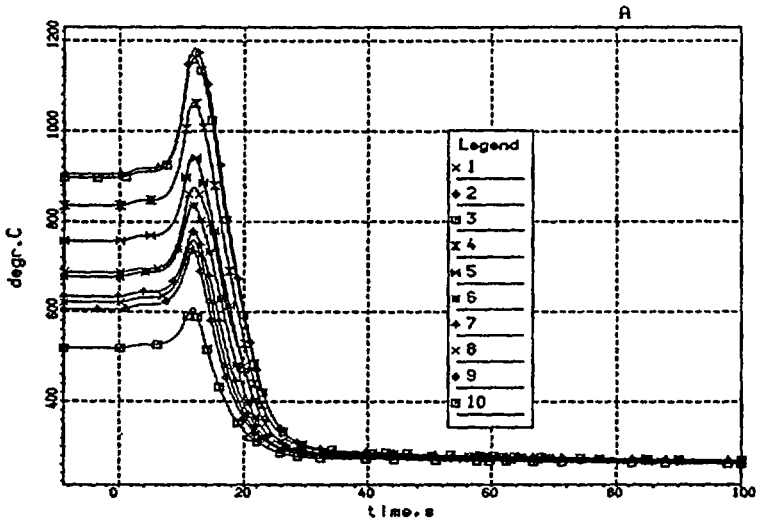

Figure 10. Maximal fuel temperature in the hottest (10 axial nodes are shown, numeration from core bottom)

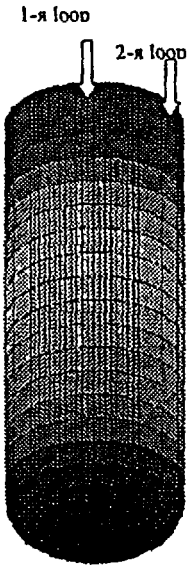

Figure 11. Down camera of the reactor

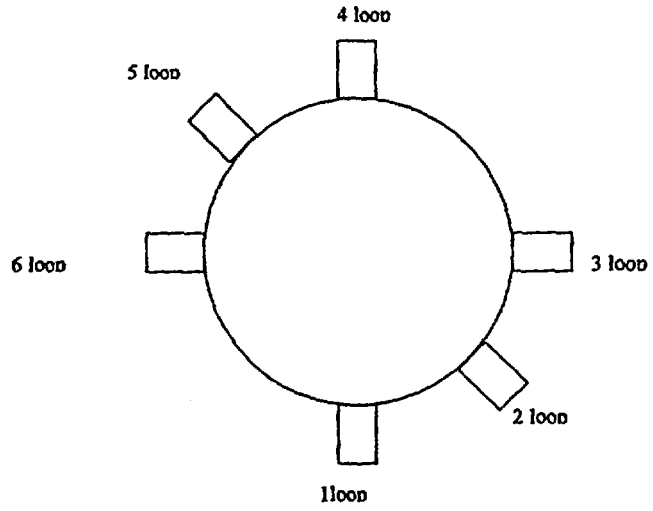

Figure 12. Connection scheme of the loops to the down camera of the reactor (the first loop is turned on)

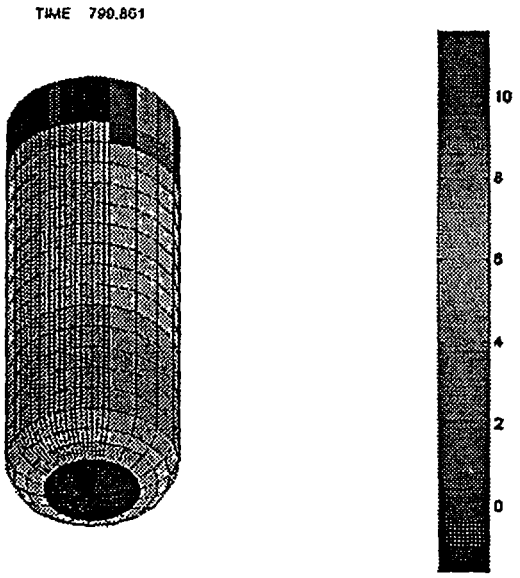

Figure 13. Coolant velocity distribution in the down camera before the transient

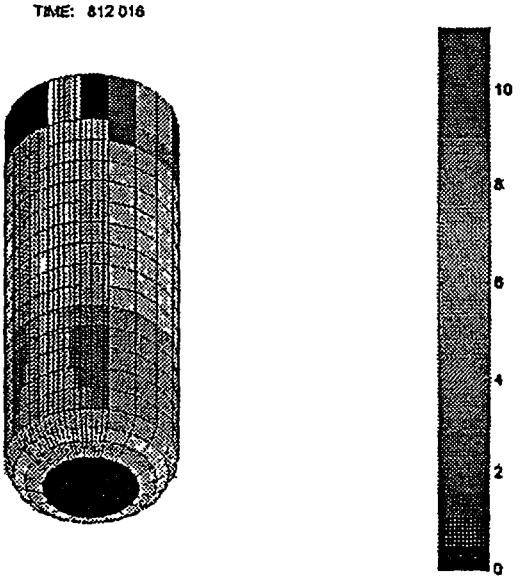

Figure 14. Coolant velocity distribution in the down camera after the transient.

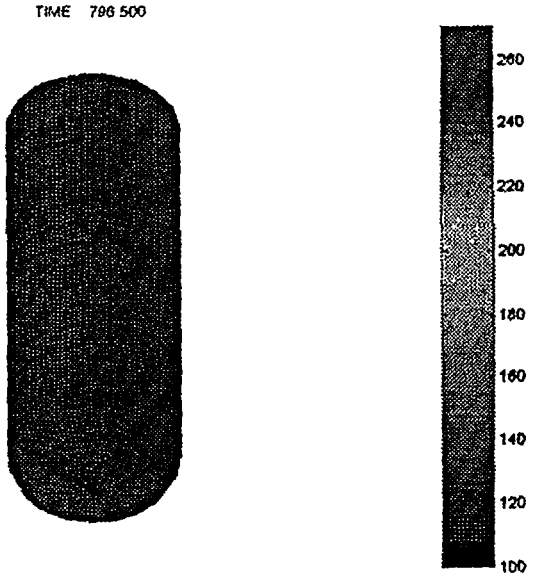

Figure 15. Coolant temperature distribution in the down camera before the transient

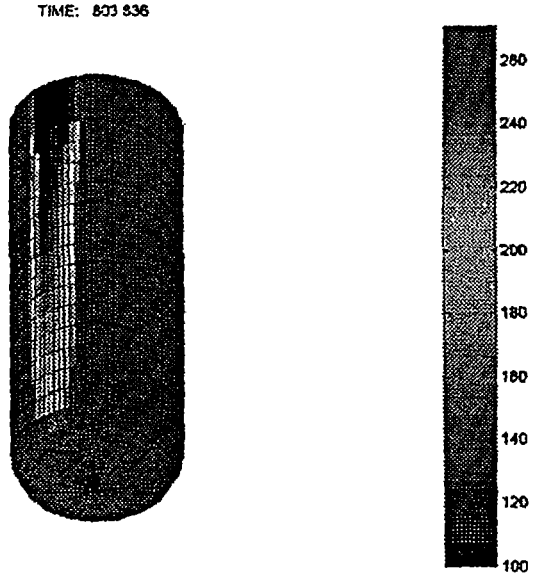

Figure 16 (1) Coolant temperature distribution in the down camera at the moment of switching on the loop

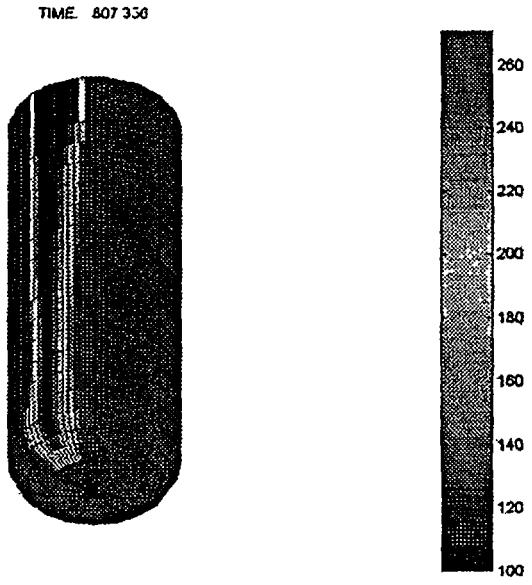

Figure 17. (2) Coolant temperature distribution in the down camera at the moment of switching on the loop

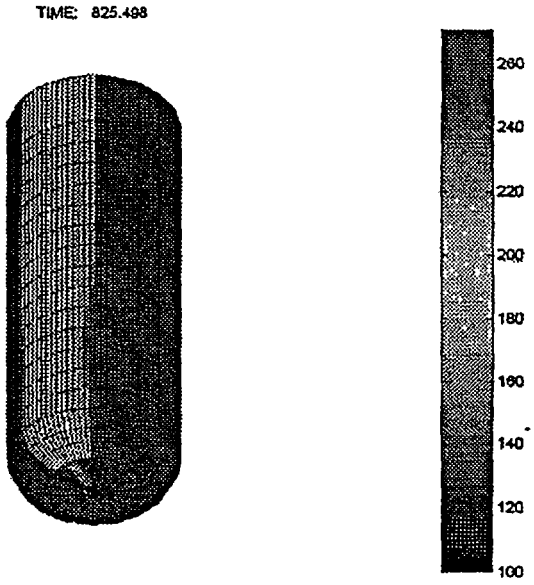

Figure 18. (3) Coolant temperature distribution in the down camera at the moment of switching on the loop.

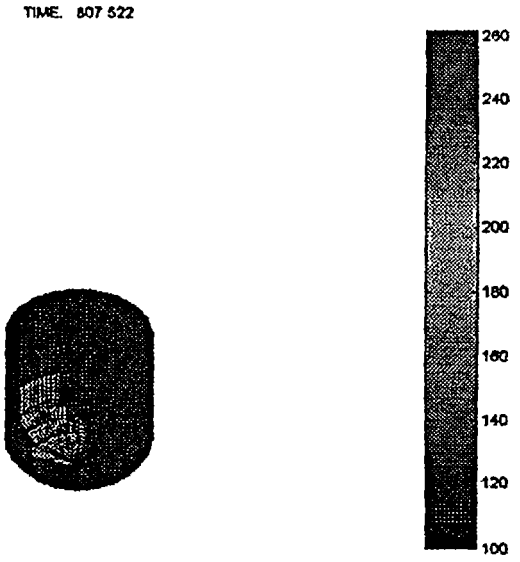

Figure 19. Coolant temperature distribution in the under-core space at the moment of switching on the loop

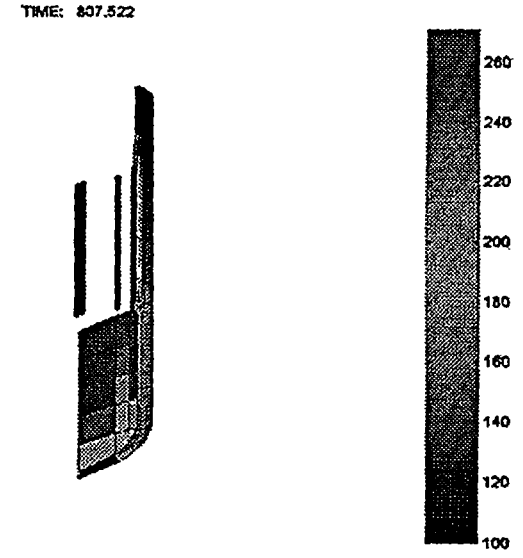

Figure 20. Coolant temperature distribution at the moment of switching on the loop in the shear of the down camera and under-core space. Some assemblies are shown (The shear is performed vertically near the plane going through the center of the first loop)

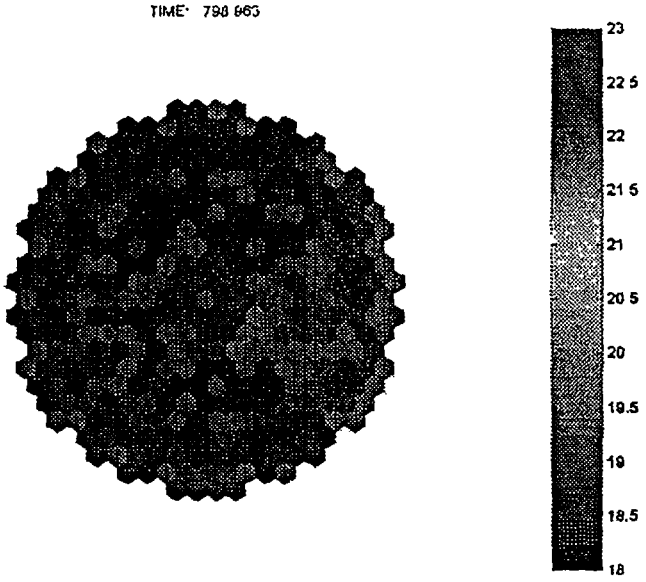

Figure 21. Mass flow distribution at the core inlet before the switching on the loop, kg/sec

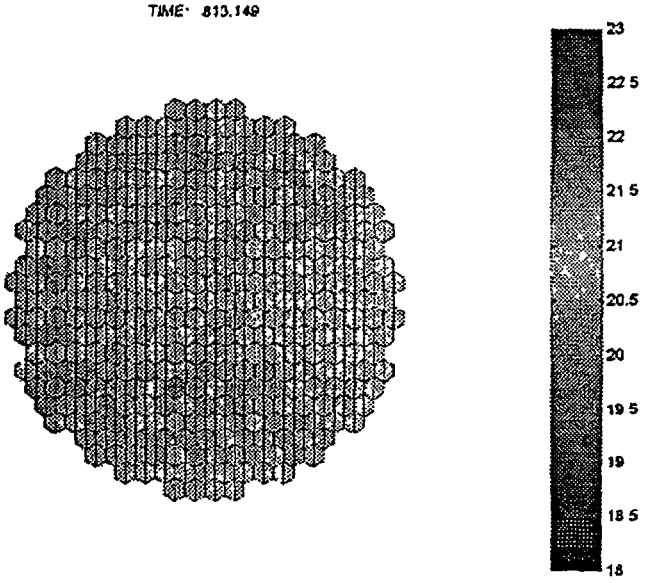

Figure 22. Mass flow distribution at the core inlet after the switching on the loop, kg/sec.

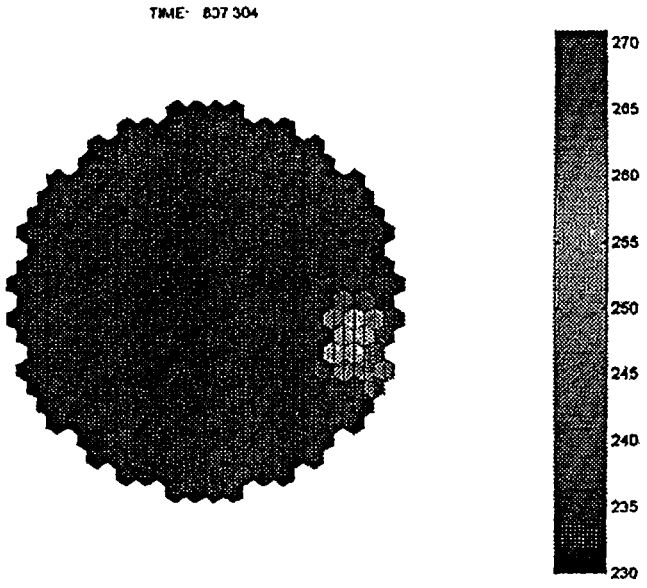

Figure 23. (1) Coolant temperature distribution at the core inlet at the time of the switching on the loop, grad C

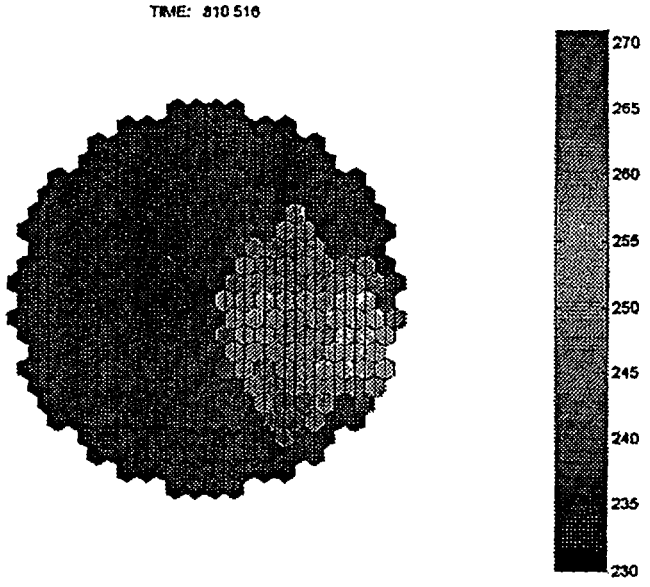

Figure 24. (2) Coolant temperature distribution at the core inlet at the time of the switching on the loop, grad C

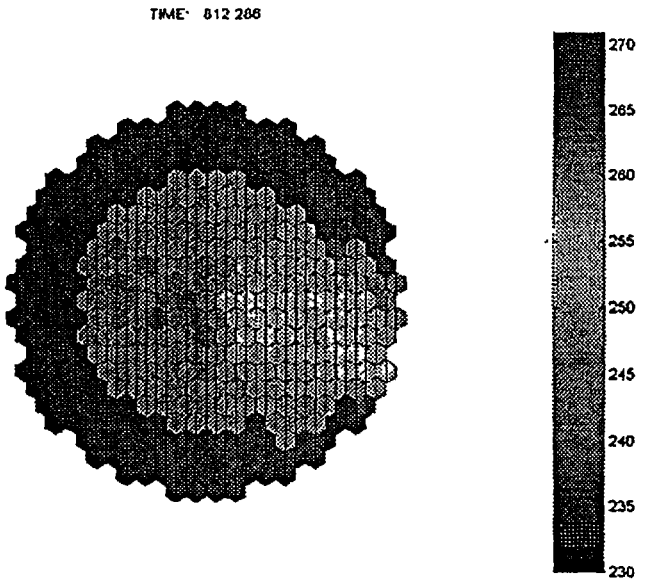

Figure 25. (3) Coolant temperature distribution at the core inlet at the time of the switching on the loop, grad C.

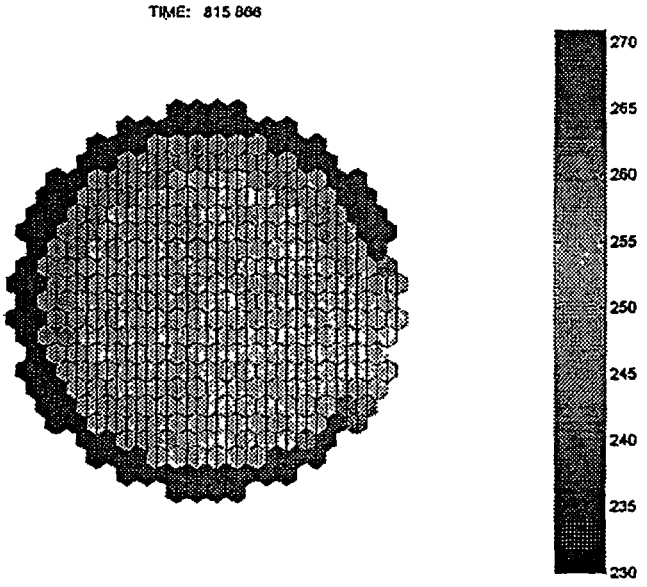

Figure 26. (4) Coolant temperature distribution at the core inlet at the time of the switching on the loop, grad C

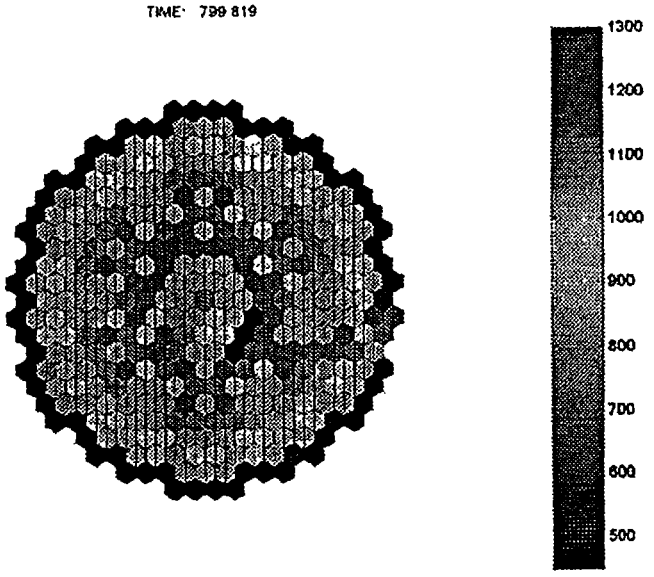

Figure 27. Distribution of center line pin fuel temperature in the core (node 3) before the switching on the loop, grad C

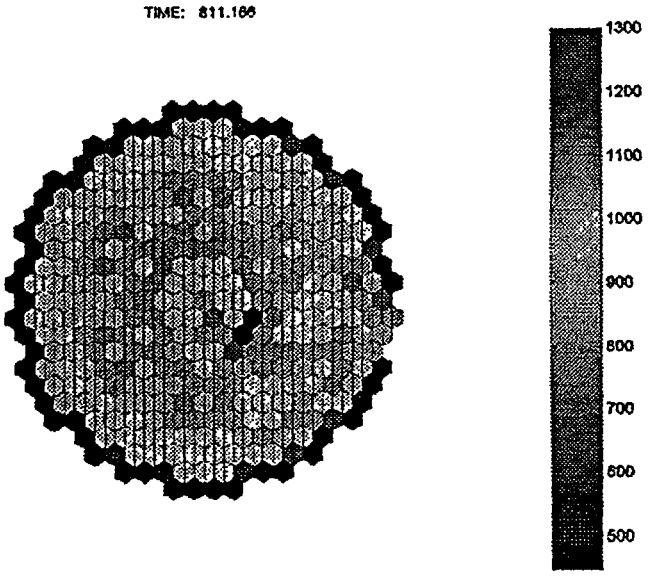

Figure 28. (1) Distribution of center line pin fuel temperature in the core (node 3) at the time of the switching on the loop, grad C

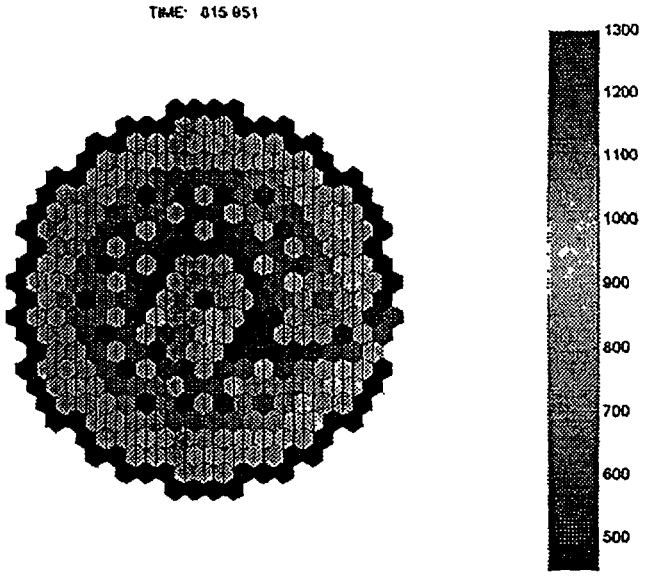

Figure 29. (2) Distribution of center line pin fuel temperature in the core (node 3) at the time of the switching on the loop, grad C

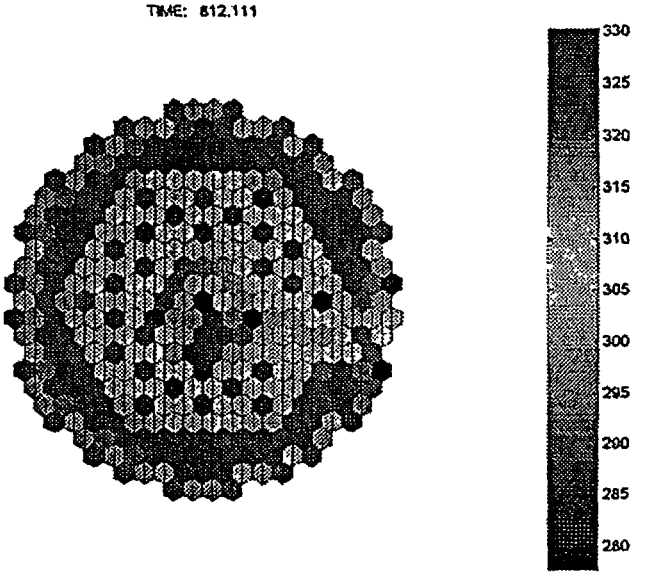

Figure 30. Distribution of center line pin fuel temperature in the core (node 9) at the time of the switching on the loop (maximum), grad C